Indian Journal of Pure & Applied Physics
Vol. 59, February 2021, pp. 125-131

Photochromic Performance of PLD grown MoO_3Thin Films

Divya Dixit & K V Madhuri*

Thin Film Research Laboratory, Division of Physics, Vignan's Foundation for Science, Technology & Research (Deemed to be University), Vadlamudi-522 213, Guntur (Dt), Andhra Pradesh, India.

Received 18 September 2020; accepted 4 December 2020

Molybdenum trioxide (MoO_3) thin films are made by Pulsed Laser Deposition (PLD) technique onto cleaned glass substrates at an oxygen partial pressure (PO_2) of 100 m Torr by varying substrate temperature (T_s). The present study describes the variation in the growth of films and photochromic properties with respect to substrate temperature. XRD studies confirm unique α - orthorhombic layered structure for grown films and the intensity of prominent peaks increases with substrate temperature. SEM images discloses that the film surface constitutes uniformly spherical grains at lower substrate temperature (T_s = 100 ℃) and turns to needle like structure as substrate temperature reaches to 200 and 300 ℃. The films deposited at 400 ℃ gives nano-crystalline structure which shows stable and high photochromic efficiency. The studies also reveal that the presence of impurities or ions on the surface of the film and effects on the photochromic performance.

Keywords: Molybdenum Trioxide thin films; PLD; Growth and photochromic properties.

1 Introduction

Transition metal oxide (TMO)'s, particularly in thin film form have drawn high consideration owing to their prospective scientific applications in the electrochromic display devices[1,2], catalyst[3], smart windows, photo-voltaic cells, lithium ion batteries *etc*[4-6]. Among these oxides, molybdenum oxide displays multifunctional properties due to its various valence states[7], high electrochemical activity, stability and less electrical resistivity[8,9]. Interaction of oxygen with molybdenum surface produces various oxidation states of molybdenum which corresponds to various phases of molybdenum oxide such as MoO_3, MoO_2, Mo_4O_{11}, $Mo_{17}O_{47}$, $Mo_{22}O_{64}$ *etc*. Amongst, molybdenum trioxide (MoO_3) has fascinating phases of structures (orthorhombic α- MoO_3 , monoclinic β-MoO_3 *etc*.), morphologies, high catalytic activity, high work function made it useful for back contact layer in solar cell, electrochemical devices, cathode based electronics, field emitters, gas sensors, optical storage devices, smart windows and switchable mirrors[10-15]. Now a days, the researchers are much more concentrating on thermodynamically stable orthorhombic phase which contains two dimensional layered structure coupled by Van der Waal forces[16,17]. The ions inserted into this layered structure increase the charge storage capacity and cause the optical modulation.

In view of applications, chromogenic technology has more concern, in which the coloration is produced by various stimuli like electric field, high energy irradiation (excitation energy is higher than energy gap), temperature *etc*. The performance of the chromogenic device absolutely depends on the growth of MoO_3 which depends critically on synthesis process. Literature survey revealed that, porous and layered structures are more responsible to change the optical properties (either transmittance or absorption) by inserting the species in the vacant sites. In earlier studies anisotropic α- MoO_3 structure has been achieved by several methods like electron beam deposition[18], thermal deposition[19], electrodeposition[20], sol-gel synthesis *etc*[21]. However, it is still a challenge to achieve an organised structure of MoO_3 with α phase. Even though, extensive research is focused on variety of applications, the researchers are not yet well understood about the photochromic process[22]. Hence the present investigation is focused to grow MoO_3 thin films with desired structure for their better and stable photochromic properties. It have also been discussed the impact of substrate temperature on the growth and photochromic performance.

2 Experimental

PLD technique is one of the versatile techniques to grow uniform and crystalline films even at low

*Corresponding author (E-mail: kvmsvu@gmail.com**)**

temperatures. Hence experimental films were grown by PLD technique (Quanta system, DNA, Laser technology) at $PO_2 \approx$ 100 mTorr by varying T_s values from 100-400 ℃. As the cleanliness is one of the criteria which effects the physical properties of the films, the chosen Corning 7059 Glass substrates were well cleaned through dipping in ethanol, iso- propyl alcohol , acetone and de-ionised water successively for 15 minutes, by using ultra sonic agitator to remove the surface contaminants. These substrates were finally blown with dry nitrogen gas and attached to the substrate holder in the vacuum chamber. Pure MoO_3 powder (Sigma Aldrich, 99.99%) was grounded into a fine powder to form pellets of one inch in diameter and 3 mm in thickness by compression at 5 ton/cm^2 and the Pellets were sintered at 400 ℃ for 2 hrs subsequently. This process was repeated twice to form highly uniform and strongly bonded pellets. The sintered pellets were used as target material and placed at a distance of 4.5 cm from the substrate. A Nd-YAG (λ= 1064 nm) pulsed laser with energy density of 300 mJ, pulse duration of 12 ns at 5Hz was used to ablate the target. The target was set to be continuously rotated to reduce the splashing effects and also to avoid the continuous deposition at the same spot. Hence, one can achieve pinhole free and uniform films during this process. In case of MoO_3, it is observed that a dark layer is formed on the target surface due to dissociation of target material by the interaction of laser beam. Hence the films deposited in the absence of oxygen seem to be dark with insignificant visibility and transparency. Hence the present investigations are carried out in presence of oxygen partial pressure, and at various substrate temperatures to vary the oxidation states of molybdenum. The laser beam is incident at an angle 45^0 to sublimate the material in the vacuum chamber which is evacuated to base pressure of $2x10^{-6}$ mbar. The flow controller measures the oxygen partial pressure (100 mTorr), temperature controller measures T_s (100-400 ℃) and thickness (200 nm) was monitored by stylus profilometer which are built in the system.

Shimadzu XRD-6000 diffractometer with CuK_α (1.542 Å) target was used for structural characterisation and topography was investigated by Scanning Electron Microscopy (SEM) (EVO-SEM MA15/18-CARLZEISS) and Atomic Force Microscopy (AFM) (NT-MDT Solver Next) in tapping mode. Optical spectra of experimental films were recorded before and after exposure to UV light by UV-VIS double beam spectrophotometer (SHIMADZU-1800). The photochromic properties were studied for the grown films by irradiating with 300 W out power radiation for different durations in the range of 5 - 60 minutes.

3 Results and Discussion

3.1. Structure - XRD Studies

Crystallographic structure of PLD grown experimental films was examined by XRD technique and the pattern was recorded in the Bragg angle range of 10^0 - 60^0 as shown in Fig. 1. XRD pattern of MoO_3 thin films prepared at T_s=100 ℃, exhibited (020), (110), (021) and (150) reflections, revealed the existence of thermodynamically stable orthorhombic layered structure of α- MoO_3. The films grow with their basal planes parallel to the surface of the substrate and the layered structure formed by sharing of MoO_6 octahedral units. The layers are formed by cross link of oxygen atoms. Further rise of substrate temperature, increases the intensity of the peaks so that crystallinity of the sample also increases due to the rearrangement of atoms and agglomeration of particles. It also enhances the adatom mobility on the surface. The study of highly intense diffraction peaks in Fig. 1 represents only α phase with layered structure. The driving forces for MoO_3 molecules to form this phase are the Van der Waal's forces in [010] direction and covalent forces in [100] and [011] directions. The interplanar spacing (calculated from Bragg's law) 'd', '2θ' and (h k l) values and corresponding JCPDS data are tabularised in Table 1. The films show crystalline nature even from T_s=100 ℃, due to high kinetic energy of ionised

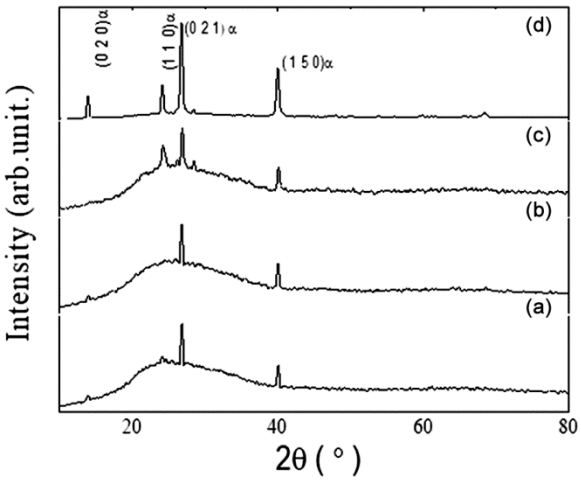

Fig. 1 — XRD pattern of PLD grown MoO_3 films at T_s (a) 100 ℃ (b) 200 ℃ (c) 300 ℃ (d) 400 ℃.

species produced in the plasma during the deposition process in PLD technique[23]. The films turn to α phase at T_s=100 ℃, as our earlier investigations on PLD grown MoO_3 thin films confirm that the films formed at substrate temperature less than 100 ℃ exhibits α-β mixed phase.

Debye - Scherrer's equation is used to calculate the average crystallite size (D) which is specified below[24]:

$$D = \frac{0.9\,\lambda}{\beta Cos\,\theta} \quad \ldots (1)$$

Where wavelength of X-ray (Cuk_α , λ =0.1546 nm) is represented as λ, Full Width Half Maximum of high intensity peak (021) is represented as β in radians and Bragg diffraction angle is denoted as θ. The calculated crystallite size is observed to be increased from 28 to 60 nm with increase of substrate temperature (till 300 ℃) and decreased to 30 nm at 400 ℃ in presence of oxygen partial pressure.

Table1 — Interplanar spacing 'd', '2θ' and (h k l) values and corresponding JCPDS data

PLD grown Molybdenum Trioxide thin films

Experimental Data		JCPDS Data	
2 **θ**(∘)	d (nm)	2 **θ**(∘)	(h k l)
13.75	0.14	12.768	(0 2 0)
24.09	0.15	23.285	(1 1 0)
26.789	0.1	27.272	(0 2 1)
39.9	0.08	39.578	(1 5 0)

3.2. Morphology

3.2.1. SEM Analysis

Figure 2 represents the microscopic images of grown films recorded by SEM. The surface feature of films observed to be homogeneous, uniform, crack free, smooth, having scattered splashed particles on the surface of the film[25]. The surface of the films consisting of uniform spherical grains for the films deposited at 100 ℃ which turns to be needle like structure with raise of substrate temperature. The grain size is increasing with increase of substrate temperature up to 300 ℃ and start decreasing at T_s= 400 ℃ due to increase in mobility of incoming molybdenum trioxide molecules[26]. The films deposited at T_s= 400 ℃ seems to be nano crystalline with reoriented spherical grains and the crystallinity is also observed to be increased which is correlated with XRD data.

3.2.2.EDS Study

The preliminary elemental analysis of the experimental films was investigated by energy dispersive spectroscopy (EDS) and the corresponding Energy Dispersive X-ray spectra is shown in Fig. 3. The set of experimental films shows only the presence of Mo and O elements, which confirms the purity of the grown films without any contaminants.

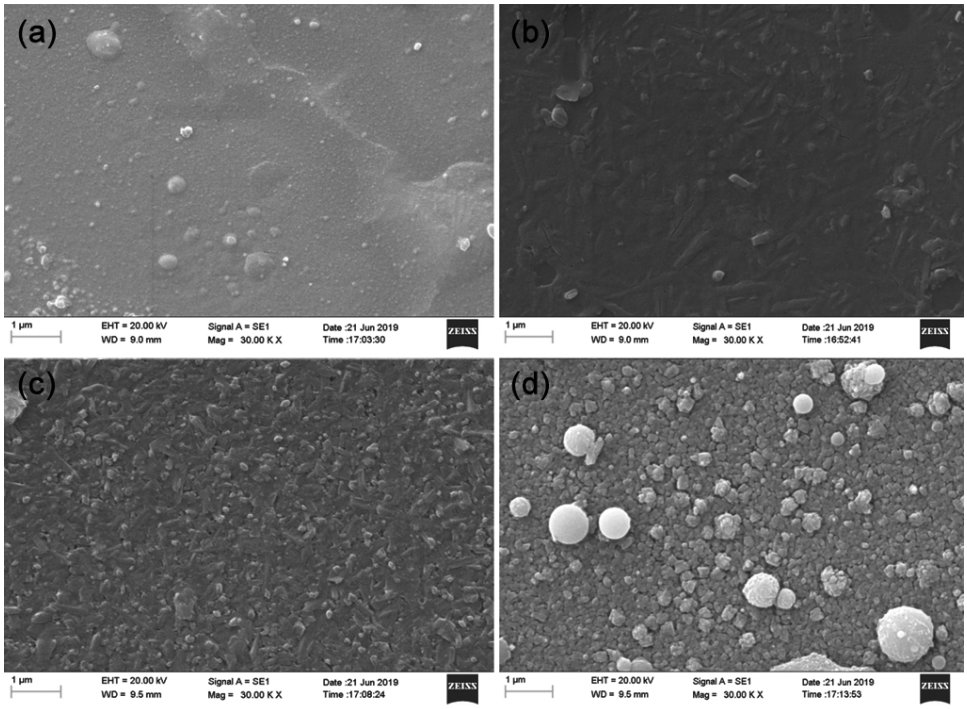

Fig. 2 — SEM Images of PLD grown MoO_3 films at T_s (a) 100 ℃ (b) 200 ℃ (c) 300 ℃ (d) 400 ℃.

3.2.3AFM Analysis

AFM images for the grown films at various substrate temperatures ranging from 100 to 400 ℃ are represented in Fig. 4(a-d). The films show fine grain spherical (in 10 μm) range which are uniformly distributed on the surface of the films. With the raise of substrate temperature the surface of the films become non uniform with agglomeration of grains till T_s reaches to 300 ℃.The surface roughness of the films seems to be increased with increase of substrate temperature. As the substrate temperature reaches to 400 ℃, the surface seems to be optically flat with small size grains which will be more effective for diffusion of light on the surface and hence to improve the photochromic properties[27].

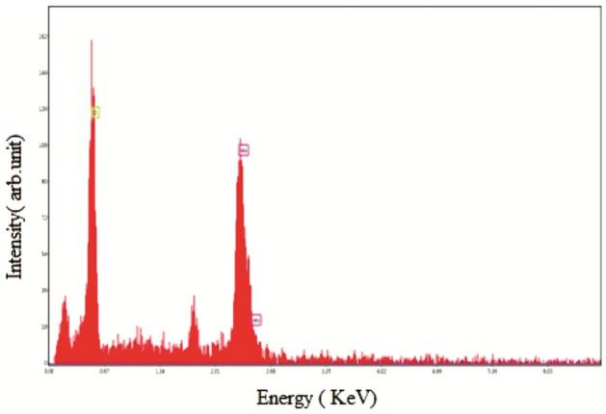

Fig. 3 — EDS of experimental MoO_3 films.

3.3.Optical Studies

Figure 5 represents the wavelength dependence of optical transmission of MoO_3 thin films deposited at PO_2 = 100 mTorr and at various substrate temperatures. Our earlier investigations revealed that the films deposited in vacuum are dark blue in colour and it changes to transparent as the oxygen flow reaches to 100 mTorr which indicates that the films approached stoichiometric MoO_3. The spectra reveal high absorption zone, before fundamental absorption

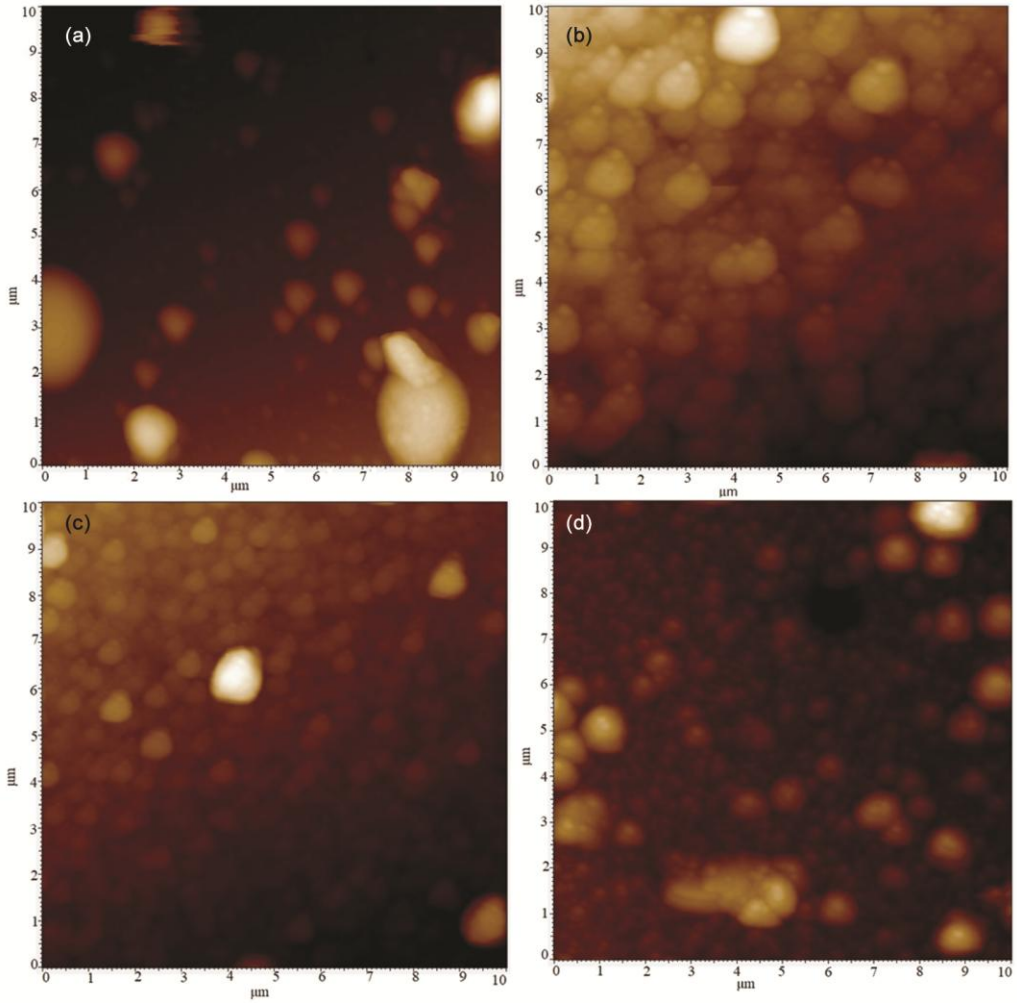

Fig. 4 — AFM Images of PLD grown MoO_3 films at T_s (a) 100 ℃ (b) 200 ℃ (c) 300 ℃ (d) 400 ℃.

edge and semi transparent zone in the wavelength range 400-1100 nm which is very useful in the determination of optical constants like thickness, extinction coefficient and refractive index. The optical absorption edge is observed for the films deposited at 100 ℃ at about 400 nm with broadband absorption in near infrared region and the optical transmittance is about 60.75 % at wavelength 478 nm. The optical transmittance is observed to be increased above the fundamental absorption edge and the absorption edge marginally moved to lower wavelength side (shows blue shift) as the substrate temperature raises to 300 ℃. Still further increase in T_s values to 400 ℃, made the thin films to be oxygen deficient with more ordered crystalline structure. The oxygen deficiency which form a defect band and is accountable for the broad band absorption. Hence, the films become sub-stoichiometric[28]. The optical transmittance for the films deposited at T_s = 400 °C was observed to be decreasing (71.78%) with some interference peaks and the fundamental absorption edge moved towards higher wavelengths (shows red shift) as shown in Fig 5(d). The films are optically flat with reduced transmission between 600-1100 nm which results due to absorption band. The optical bandgap was calculated from the transmittance data where the reflection losses were taken into account. The optical absorption co-efficient (α) of the grown films was estimated with the help of following relation,

$$\alpha = - (1/t) \ln (T) \quad \ldots (2)$$

Where optical transmittance is represented by 'T' and film thickness is denoted by 't'. By using Tauc's relation[29] given in equation (3), the optical bandgap (E_g) and type of transition (basing on 'n' value) is evaluated from the optical absorption co-efficient.

$$(\alpha h\nu) = B(h\nu - E_g)^n \quad \ldots (3)$$

Figure 6 shows the plots of $(\alpha h\nu)^2$ Vs photon energy (hν) and the plots gave a better fit for n=1/2 which represents direct allowed transition, and extrapolation of the linear portion gives the optical bandgap of the grown films. The optical band gap (E_g) is observed to be increased from 3.23 to 3.47 eV with the raise of substrate temperature. On the other hand, for the films grown at T_s = 400 ℃, bandgap decreased to 3.29 eV. The optical bandgap is in the range of 3.2 to 3.7 eV[30,31] which is in good agreement with polycrystalline α-MoO_3 in both powder and thin film form. The variation of optical bandgap with substrate temperature is shown in Fig. 7.

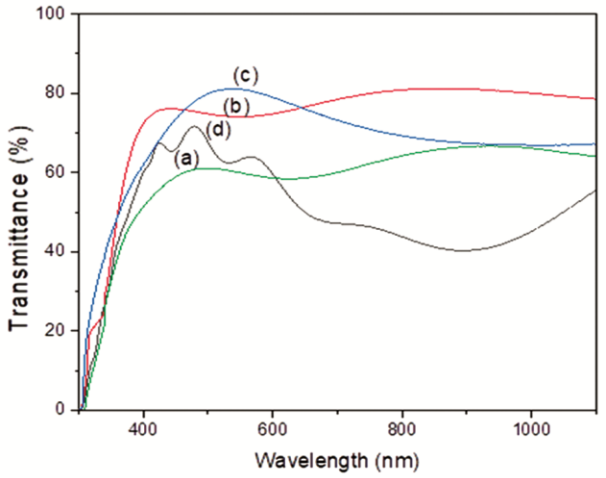

Fig. 5 — Transmittance variation with wavelength for PLD grown MoO_3 films at T_s (a) 100 ℃ (b) 200 ℃ (c) 300 ℃ (d) 400 ℃.

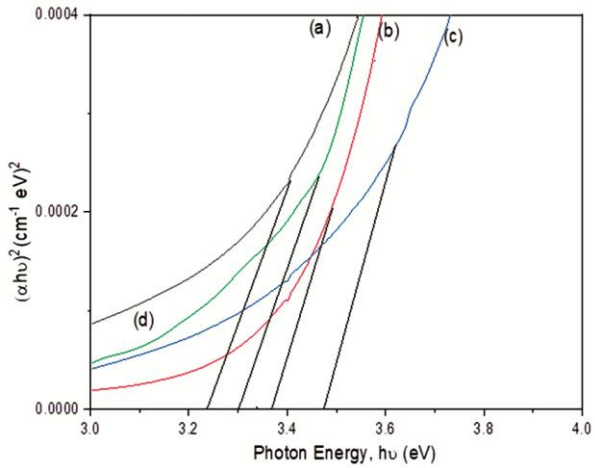

Fig. 6 — $(\alpha h\nu)^2$ Vs hν plots for PLD grown MoO_3 films at T_s (a) 100 ℃ (b) 200 ℃ (c) 300 ℃ (d) 400 ℃.

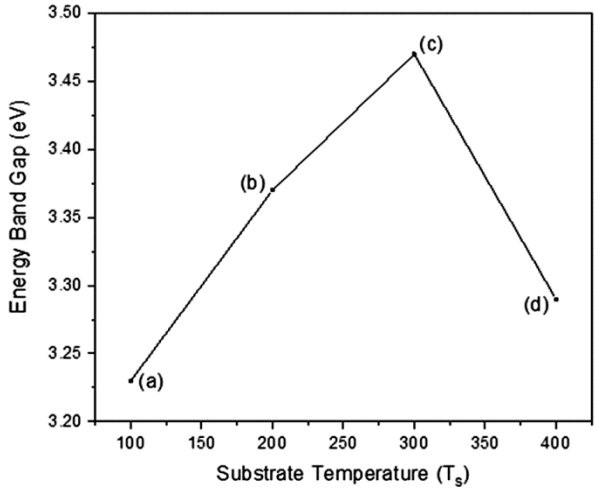

Fig. 7 — Variation of Bandgap with substrate temperature for Molybdenum Trioxide thin films.

3.4. Photochromic Studies

The transmittance of the films in the bleached state displays high transmission in the visible region and the surface of the films are optically flat. The large grain size supresses the interference effect for the films grown up to 300 ℃. As the films deposited at T_s= 400 ℃ are nanocrystalline nature, the films show interference peaks in the bleached state.

The grown films were exposed to UV radiation to study the photochromic properties in which the prime objective is to monitor the changes in the oxidation states of molybdenum due to the interaction with UV radiation and correlate these changes to colour change. The transmittance spectra before and after the exposure to UV radiation for various duration of timings are shown in Fig. 8. When the films were exposed to radiation, electrons are got excited to the conduction band by leaving the same number of holes in the valence band which is explained by the equation below:

$$MoO_3 + hv \rightarrow MoO_3 + e^- + h^+ \quad \ldots (4)$$

Holes oxidize the water molecule which is present on the surface of the films at the time of deposition[32].

$$H_2O + 2h^+ \rightarrow 2H^+ + O \quad \ldots (5)$$

The electrons which are generated by the above process, occupies the vacancies and form bronze ($H_xMo_{1-x}^{VI}Mo_x^{V}O_3$). Similarly, the oxidation of state also changed which causes the colour change in the films and as well as the optical transmittance and hence the colour turns to blue. As the time of exposure increases, the creation of electron-hole pair is also increased which turns more chances of formation of bronze.

$$MoO_3 \text{ (clear)} + xH^+ + xe^- \rightarrow H_x\, Mo^{VI}_{1-x}\, Mo^{V}_{x}\, O_3 \text{ (bluish)} \quad \ldots (6)$$

$$Mo^{VI}_A + Mo^{V}_B + hv \rightarrow Mo^{V}_A + Mo^{VI}_B \quad \ldots (7)$$

By the absorption of light radiation, the transfer of electrons is possible between Mo^V and Mo^{VI} sites. The optical density ΔOD is calculated by taking the logarithmic ratio of transmittance in bleached state to coloured state. The colouration is found to be more at $\lambda \approx 479.48$ nm for the films deposited at T_s=400 ℃, which confirms the nanocrystalline structure promotes enhancement in photochromic

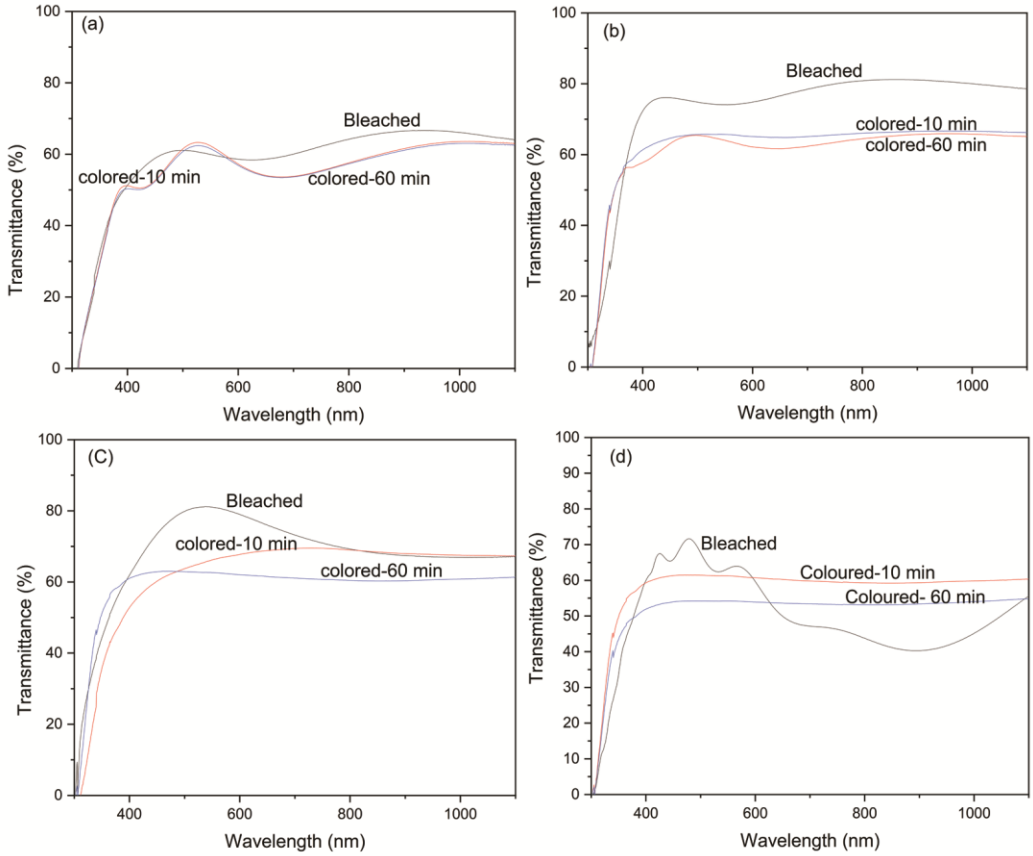

Fig. 8 — Optical transmittance variation with UV irradiation of PLD grown MoO_3 films.

properties[33]. This favours that microstructure and oxygen deficiencies in the grown films take a vital role in the photochromic efficiency than the surface water molecules[34].

4 Conclusion

The experimental MoO_3 films were deposited by PLD technique at various substrate temperatures ranging from 100 to 400 ℃ under oxygen atmosphere. The films showed unique orthorhombic layered structure, with thermodynamically stable α-phase. The films are found to be pure with the presence of spherical uniform grains initially and turns to needle like structure at T_s=200 ℃ and 300 ℃. The films deposited at T_s=400 ℃ turn to nano-crystalline structure. The optical transmittance of films gave a better fit for direct allowed transitions and the band gap varied from 3.23 to 3.47 eV. The films grown at T_s=400 ℃, shows better photochromic efficiency due to its nanocrystalline structure and oxygen deficiencies present in the film.

References

1 Faughnan B W & Crandall R S, *Appl Phys Lett*, 31 (1977) 834.
2 Chernova N A, Roppolo M, Dillon A C & Whittingham M S, *J Mater Chem*, 19 (2009) 2526.
3 Pham T T P, Nguyen P H D, Vo T T, Nguyen H H P & Luu C L, *Adv Nat Sci : Nanosci Nanotechnol*, 6 (2015) 045010.
4 Mai L, Yang F, Zhao Y, Xu X, Xu L, Hu B, Luo Y & Liu H, *Mater Today*, 14 (2011) 346.
5 Chen W, Mai L, Qi Y & Dai Y, *J Phys Chem Solids*, 67 (2006) 896.
6 Li D, Liu Y, Lin B, Lai C, Ying S, Hong Y & Xueqin Z, *RSC Adv*, 5 (2015) 98278.
7 Ashrit P, *Transition Metal Oxides Thin Film Based Chromogenics and Devices*, (Elsevier), 2017.
8 Ramana C V & Julien C M, *Chem Phys Lett*, 428 (2006) 114.
9 Aoki T, Matsushita T & Mishero K, *Thin Solid Films*, 517 (2008) 1482.
10 Xia Q, Zhao H, Du Z, Zeng Z, Gao C, Zhang Z, Du X, Kulka A & Konrad S, *Electrochim Acta*, 180 (2015) 947.
11 Andersson A M, Granqvist C G & Stevens J R, *Appl Opt*, 28 (1989) 3295.
12 Granqvist C G, *Solid State Ionics*, 53 (1992) 479.
13 Ferroni M, Guidi V, Martinelli G, Nelli P, Sacerdoti M & Sberveglieri G, *Thin Solid Films*, 307 (1997) 148.
14 Al-kandari H, Al-khorafi F, Belatel H & Katrib A, *Cataly Commun*, 5 (2004) 225.
15 Mutschall D, Holzner K & Obermeier E, *Sens Actuator B*, 36 (1996) 320.
16 Sunu S, Prabhu E, Jayaraman V, Gnanasekar K, Seshagiri T & Gnanasekaran T, *Sens Actuators B*, 101 (2004) 161.
17 Li G, Li J, Pang S, Peng H & Zhang Z, *J Phys Chem B*, 110 (2006) 24472.
18 Sivakumar R, Gopalakrishnan R, Jayachandran M & Sanjeeviraja C, *Current Appl Phys*, 7 (2007) 51.
19 Sian T S & Reddy G B, *Solar Energy Mater Solar Cells*, 82 (2004) 375.
20 Liu S, Zhang Q, Wang E & Dong S, *Electrochem Commun*, 1 (1999) 365.
21 Jiebing S & Rui X, *J Sol-Gel Sci Technol*, 27 (2003) 315.
22 Allogho G G & Ashrit P V, *Thin Solid Films*, 520 (2012) 2326.
23 Al-Kuhaili M F, Durrani S M A & Bakhtiari I A, *Appl Phys A*, 98 (2010) 609.
24 Scofield J H, Duda A, Albin D, Ballard B & Predecki P, *Thin Solid Films*, 260 (1995) 26.
25 Camacho-Lopez M A, Escobar-Alarcon L & Haro-Poniatowski E, *Appl Phys A*, 78 (2004) 59.
26 Sharma R K & Reddy G B, *J Alloys Comp*, 598 (2014) 177.
27 Nirupama V & Uthana S, *J Mater Sci:Mater Electron*, 21 (2010) 45.
28 Subbarayudu S, Madhavi V & Uthanna S, *Int J Mater Sci (IJMSCI)*,4 (2014) 78.
29 Tauc J, *Amorphous and Liquid Semiconductors*, Springer, London and New York, (1974).
30 Navas I, Vinodkumar R, Lethy K J, Detty A P, Ganesan V, Sathe V & Mahadevan Pillai V P, *J Phys D: Appl Phys*, 42 (2009) 175305.
31 Elangovan E, Goncalves G, Martins R & Fortunato E, *Solar Energy*, 83 (2009) 726.
32 He T, Ma Y, Cao Y, Jiang P, Zhang X, Yang W & Yao J, *Langmuir*, 17 (2001) 8024.
33 Li S & Samy E S M, *Nano Struct Mater*, 12 (1999) 215.
34 Beydaghyan G, Doiron S, Haché A & Ashrit P V, *Appl Phys Lett*, 95 (2009) 051917.